

## THE INFLUENCE OF ACID DIFFUSION ON THE PERFORMANCE OF LEAD-ACID CELLS

W. KAPPUS and J. BOHMANN

VARTA Batterie AG, Forschung und Entwicklung, Gundelhardtstrasse 72, D-6233 Kelkheim (Taunus) (F.R.G.)

(Received March 10, 1983; in revised form July 30, 1983)

### Summary

A model for the discharge performance of the lead-acid cell is proposed. Diffusion of acid into the porous electrodes, which is connected with diffusional polarization, is considered as the principal factor in the transport process. The end of discharge is determined either by acid depletion inside the electrodes or by exhaustion of the active material, where utilization of the active material as a function of the acid density and the specific current is determined from empirical expressions.

Curves of diffusional polarizations as a function of the discharge time are presented. Calculated discharge capacities show the influence of various parameters such as electrode thickness, current, and acid density. Tubular and pasted plates are considered.

---

### 1. Introduction

The lead-acid cell is expected to be the most important secondary battery for at least another 10 to 20 years [1] and is still an object of intensive research. In this context, a mathematical modelling of the lead-acid cell can be useful both for the solution of technical problems and for a deeper insight into the processes determining the performance of the cell.

In principle, the performance of the cell depends on its different constituents: positive and negative grids, positive and negative active material, electrolyte, separator, etc. Under different conditions any one of these factors may become important or even dominant and may be optimized. For example, much work has been done on the optimization of the grid design to reduce the grid mass and the ohmic losses in the cell [2]. The present article concentrates on the influence of the porous structure of the electrodes on the discharge capacity.

In general, the charge and discharge reactions of both the  $\text{Pb}/\text{PbSO}_4$  and the  $\text{PbO}_2/\text{PbSO}_4$  electrode are influenced by the transport of matter and electricity, and by the volume changes of the different phases. The com-

plicated interrelation of these processes, and their dependence on the space coordinates and the time, has to be accounted for by a "theory of porous electrodes". In practice, however, it is impossible to describe all the features of the electrodes exactly, especially is it not possible to treat the different geometries of all the single pores, and simplifying models are therefore necessary.

A model in common use is the "macrohomogeneous model" where the solid and the liquid phases are assumed to be continuously distributed and to be superposed independently. Physical quantities are described by functions defined by appropriate averaging processes. Most of the literature up to 1974 was reviewed by Newman and Tiedemann [3] who also discussed applications to batteries. A detailed treatment of the porous  $\text{PbO}_2/\text{PbSO}_4$  electrode, in which the formation of water during the discharge reaction was especially taken into account, was given by Micka and Roušar [4, 5]. The theory of porous electrodes with respect to the  $\text{Pb}/\text{PbSO}_4$  electrode was covered by an article by Hampson and Lakeman [6]. On the basis of the equations derived by Stein [7] and Lehning [8], Horváth considered the effects of the local change of porosity and of the effective conductivity of the porous active material [9]. The results were applied to a tubular positive  $\text{PbO}_2$  electrode. A recent paper on the lithium-aluminium, iron sulfide battery [10] may serve as an example of other electrochemical systems which have been analyzed by means of this model.

The general formulations of the macrohomogeneous model cited above lead to complicated systems of partial differential equations with several free parameters, for which analytical solutions cannot be given. Therefore, approximations must be introduced or numerical techniques using fast computers must be applied. On the other hand, it is desirable for technical problems to have a model which can be easily handled; so we sought for simplifications whilst retaining the most important features, especially those affecting the discharge capacity.

Two factors which limit the discharge capacity are considered in this article: acid depletion, and exhaustion of the active material.

(i) Acid depletion can occur due to the fact that inside the porous electrodes  $\text{SO}_4^{2-}$ -ions are consumed by the discharge reaction and their replenishment by diffusion, migration, and electrolyte flow is limited. In the present paper transport of acid is described only by diffusion. The effects of migration and flow of electrolyte are approximately taken into account by the use of an effective diffusion coefficient.

Under these simplifying assumptions the resulting equations can be solved exactly for steady state conditions. The boundary conditions, however, must be treated numerically. Based on these solutions, the discharge reaction is described by a series of quasi-stationary processes with the end of discharge being defined by a critical polarization.

(ii) For a discussion of the different factors which can lead to exhaustion of the active material we refer to another article [11]. The most important influences are the acid concentration, the current density, and the

temperature, as was demonstrated for the "PbSO<sub>4</sub>-passivation" [12]. The effects of current density and acid density are introduced into the present model by empirical functions derived from "eloflux" experiments [13].

Good approximations for the discharge capacity are obtained, provided the discharge rate is not too high.

## 2. The model

Before we start the discussion of our model, we introduce a convention used throughout the article: by application of Faraday's law for a two-electron process, amounts of the active materials as well as amounts of electricity are given in (the units of) A h. Concentrations, currents, diffusion currents, etc., are accordingly defined in the practical A, h, cm system.

### 2.1. The model cell

The model cell is defined by a number of  $n_+$  positive and  $n_-$  negative plates, the acid volume  $V_a$ , the acid density,  $\rho$ , and the volume of inactive acid  $V_s$ , which allows for the fact that acid in certain regions of the cell is not involved in the discharge process. The electrodes are characterized by their length  $l$ , width  $b$ , and by the electrode thickness  $2d$  for pasted plates, or the tube and spine radii  $r_i$  and  $r_s$  for tubular plates. In the case of tubular plates the number of tubes in the plate,  $n_t$ , must also be given. The capacity of the cell may be limited by either of the two polarities. Only the total amount of active material,  $G$ , of the capacity limiting polarity has to be fixed.

The cell defined by these parameters is represented by only one plate of the limiting polarity. To this plate belongs an acid volume  $V_e$  given by the total volume of active acid divided by twice the number,  $n$ , of plates of this polarity,

$$V_e = (V_a - V_s)/2n \quad (1)$$

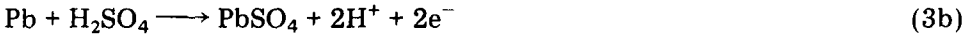
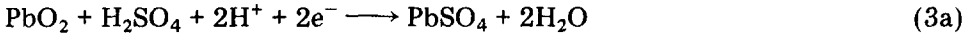
In the case of tubular plates the active material is surrounded by the tube walls of thickness  $\delta_s$ . In the case of pasted plates  $\delta_s$  is the thickness of the separator adjacent to the active material. The volume porosity of the active material at every state of discharge is calculated from the amounts of the different solid phases, their densities, and the geometric data of the plate.

### 2.2. The discharge model

The discharge is characterized by a constant current,  $I$ , per cell, which is assumed to be equally distributed over the plates of the limiting polarity. Thus the discharge current for the representative electrode  $I_e$  is given by

$$I_e = I/n \quad (2)$$

The discharge current is due to electrochemical reactions, which for the positive and the negative electrode are described by the equations



From these equations it is evident that  $\text{SO}_4^{2-}$ -ions are consumed by the discharge reactions; the acid concentration inside the porous electrodes decreases. To enable further discharge, acid has to be transported into the electrodes from the space between the plates. The balance between consumption and transport of acid is crucial for the discharge behaviour of the lead-acid cell.

In general, ohmic drops in the grids and the active materials lead to inhomogeneous distributions of current densities over the geometric surface of the plates. However, if the discharge rates are not too high these effects are negligible and physical quantities may be assumed to differ only in the direction orthogonal to the surface. This direction is characterized by the generalized coordinate  $z$ , and the different regions considered in the model are sketched in Fig. 1.

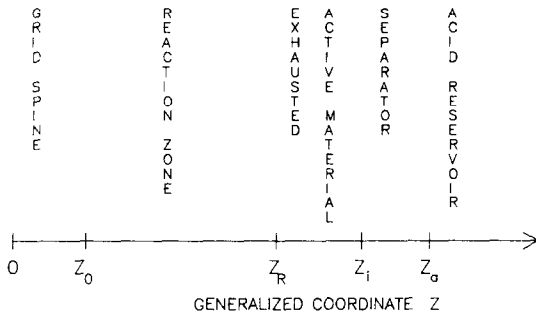


Fig. 1. Diagrammatic representation of the one-dimensional discharge model.

The spine ( $0 \leq z < z_0$ ) is only considered in the case of tubular plates. In the reaction zone ( $z_0 \leq z < z_R$ )  $\text{PbO}_2$  or  $\text{Pb}$  is transformed to  $\text{PbSO}_4$ ,  $\text{SO}_4^{2-}$ -ions are consumed and acid is transported in the fluid phase. The zone of exhausted active material ( $z_R \leq z < z_i$ ) accounts for the fact that, due to inhomogeneous (with respect to the coordinate  $z$ ) reaction rates, the outer part of the active material may be completely discharged while discharge can still go on in the inner part. In this zone, as well as in the separator ( $z_i \leq z < z_a$ ), only transport of electrolyte has to be considered. Within the acid reservoir ( $z_a \leq z$ ) a homogeneous acid concentration due to convection is assumed; the concentration is only a function of time.

Assuming that the balance of acid dominates the discharge performance of the electrodes of the lead-acid cell we have to describe two processes: acid consumption according to the reactions (3) and transport of acid.

Different processes contribute to the transport of acid.

(i) Equations (3) show that the amounts of the solid phases in the porous electrodes are changed by the discharge reactions. This results in a decrease of the volume porosity. Additionally, the amount of electrolyte is

affected; this is especially important for the positive electrode, where water is formed. In general, these effects lead to a flow of electrolyte out of the porous electrode.

(ii) The current flowing through the electrolyte results in migrational transport of acid.

(iii) The discharge reaction causes a concentration gradient from the internal part of the electrode to the acid reservoir leading to diffusion of  $\text{H}_2\text{SO}_4$ . A complete account of these processes has been given in the literature [3 - 5].

As the transference number of sulphate ions in sulphuric acid is low, mass transport by migration may be ignored. Electrolyte convection is also not considered explicitly in the present model. These two processes are approximately accounted for by the use of an effective diffusion coefficient.

In the different regions of the electrode sketched in Fig. 1 diffusion occurs in porous bodies of different porosities  $\pi_j$  (the subscript  $j$  is used to distinguish between the different regions). For the effective diffusion coefficient  $D_j$  we write

$$D_j = D_0 \pi_j^\gamma \quad (4)$$

$D_0$  and  $\gamma$  are treated as adjustable parameters and are assumed to comprise the effects of migration and electrolyte flow.

With these definitions we are ready to write down the differential equations that describe the acid balance in our model electrode. In the reaction zone characterized by the subscript R, the dependency on the time  $t$  and the coordinate  $z$  of the  $\text{SO}_4^{2-}$ -concentration  $c_R$  is governed by

$$\frac{\partial c_R}{\partial t} - D_R \nabla^2 c_R = -k_1 c_R + k_0; \quad z_0 \leq z < z_R \quad (5)$$

The second term on the left-hand side accounts for the diffusion. The right-hand side is just the Butler-Volmer expression for the electrochemical reaction step, where the kinetic constants  $k_0$ ,  $k_1$  are related to the usual formulation by

$$k_0 = i_0 \exp\{2F\eta\alpha/RT\}, \quad (6)$$

$$k_1 = (i_0/c_0) \exp\{-2F\eta(1-\alpha)/RT\} \quad (7)$$

In the zone of exhausted active material ( $z_R \leq z < z_1; j = e$ ) and in the separator ( $z_1 \leq z < z_a; j = s$ ) the reaction term vanishes and we are left with

$$\frac{\partial c_j}{\partial t} - D_j \nabla^2 c_j = 0 \quad (8)$$

The homogeneous acid concentration in the acid reservoir  $c_r$  as a function of time can be calculated from

$$\frac{\partial c_r}{\partial t} = - \frac{2bl}{V_r} D_s \nabla c_s \Big|_{z=z_a} \quad (9)$$

where  $V_r$  is the volume  $V_e$  defined by eqn. (1) minus the pore volume of the electrode in the fully charged state.

The description of the acid balance during discharge is completed by fixing the boundary conditions for the concentrations

$$c = c_0; \quad t = 0; \quad z \geq z_0 \quad (10a)$$

$$c_R(z_R) = c_e(z_R); \quad t \geq 0 \quad (10b)$$

$$c_e(z_i) = c_s(z_i); \quad t \geq 0 \quad (10c)$$

$$c_s(z_a) = c_r; \quad t \geq 0 \quad (10d)$$

and the fluxes

$$D_R \nabla c_R|_{z=z_0} = 0; \quad t \geq 0 \quad (11a)$$

$$D_R \nabla c_R|_{z=z_R} = D_e \nabla c_e|_{z=z_R}; \quad t \geq 0 \quad (11b)$$

$$D_e \nabla c_e|_{z=z_i} = D_s \nabla c_s|_{z=z_i}; \quad t \geq 0 \quad (11c)$$

The solution  $c(z, t)$  of this set of equations enables the following balance equation to be formulated:

$$\frac{d}{dt} \int dv c(z, t) = I \quad (12)$$

where the range of integration extends over the entire electrolyte volume associated with the electrode. We note that inside the porous electrode only the free pore volume contributes to this integral.

Since we are now able to describe the acid balance during discharge, we have next to consider the balance of the active material. The right-hand side of eqn. (5) is identical to the local reaction current per volume of the porous electrode  $i(z, t)$ . According to eqns. (3) this reaction current is associated with a consumption of active material and thus leads to a decrease of the local residual capacity per volume  $u(z, t)$  and of the porosity. Before discharge the active material is characterized by a homogeneous capacity per volume  $u_0$ . As was shown in another article [13], the extent to which this capacity can be used depends on the acid concentration and on the reaction current. The local residual capacity is described by the following equation:

$$u(z, t) = u_0 - \int_0^t d\tau i(z, \tau)/f(i, c) \quad (13)$$

where the influences of the acid density and the reaction current reported in ref. 13 are covered by the utilization factor

$$f(i, c) = \frac{1}{1 + \nu i(z, t)} \frac{2Y}{1 + Y^2}; \quad Y = c(z, t)/c^* \quad (14)$$

The constants  $\nu$  and  $c^*$  are characteristic of the positive and the negative active material. Local exhaustion of the active material obviously is defined by  $u(z, t) = 0$ .

Due to the transformation of  $\text{PbO}_2$  or  $\text{Pb}$  to  $\text{PbSO}_4$  during discharge, the porosity of the active material changes. As an approximation we assume that the porosity of the active material,  $\pi_R$ , is homogeneous over the reaction zone. Before discharge this porosity is  $\pi_R^0$  and it changes according to the equation:

$$\frac{d\pi_R}{dt} = -\Delta V I_e / V_R, \quad (15)$$

where  $\Delta V$  is the change in solid phase volume per A h of discharged capacity and  $V_R$  is the volume of the reaction zone.

### 3. Calculation of discharge capacities

Unfortunately, there is no known simple solution of eqns. (5), (8) and (9) subject to the boundary conditions eqns. (10) and (11). Therefore, the development of the acid concentration in time and space cannot be given in closed form for our model. Analytical solutions can however be found for steady state conditions. The steady state approximation, which is used throughout the present calculations, is reasonable as long as the characteristic time of the transient part of the time dependent solution is small compared with the discharge time.

#### 3.1. Steady state solutions

For steady state conditions ( $\partial c / \partial t = 0$ ) the reaction-diffusion equation simplifies to

$$D_R \nabla^2 c_R - k_1 c_R + k_0 = 0 \quad (16)$$

Using the new variable

$$y = c_R - k_0/k_1 \quad (17)$$

we obtain

$$\nabla^2 y - \frac{k_1}{D_R} y = 0; \quad z_0 \leq z < z_R \quad (18)$$

In the zone of exhausted active material and in the separator we are left with

$$\nabla^2 c_j = 0 \quad (19)$$

In the steady state case, in addition to the boundary conditions, eqns. (10) and (11), the equation

$$-D_R \nabla c = \frac{I_e}{A(z)}; \quad z_R \leq z < z_a \quad (20)$$

holds, *i.e.*, the diffusion flux of sulphuric acid in the non-reaction zones does not change with time and is proportional to the discharge current. The

proportionality constant  $A$  is an area, which depends on the geometry of the electrode. Two different geometries are considered here: plane geometry (pasted plates) and cylindrical geometry (tubular plates).

### 3.1.1. Pasted electrodes (flat plates)

In the case of a pasted plate the appropriate coordinate is the cartesian coordinate  $x$  perpendicular to the geometric surface of the plate; for reasons of symmetry, the origin of the coordinate system is placed in the middle of the plate and only one half of the plate ( $x \geq 0$ ) is considered in the following calculations. The Laplace operator is then

$$\nabla^2 = \frac{\partial^2}{\partial x^2} \quad (21)$$

and thus the differential equations defining the steady state process are:

$$\frac{\partial^2 y}{\partial x^2} - \frac{k_1}{D_R} y = 0 \quad x_0 \leq x < x_R \quad (22)$$

$$\frac{\partial^2 c_e}{\partial x^2} = 0 \quad x_R \leq x < x_i \quad (23)$$

$$\frac{\partial^2 c_s}{\partial x^2} = 0 \quad x_i \leq x < x_a \quad (24)$$

The surface area  $A$  (see eqn. (20)) in this case is not a function of  $x$  and is two times the geometric surface of the plate:

$$A = 2lb \quad (25)$$

In our approximation the influence of the grid on the diffusion process is neglected, *i.e.*,  $x_0 = 0$ .

After some elementary calculations the following equations for the acid concentration as a function of the coordinate  $x$  are obtained:

$$c_s = c_r + \frac{I_e}{2lbD_s} (x_a - x) \quad x_i \leq x < x_a \quad (26)$$

$$c_e = c_r + \frac{I_e}{2lb} \{ (x_a - x_i)/D_s + (x_i - x)/D_e \} \quad x_R \leq x < x_i \quad (27)$$

$$c_R = \{ c(x_R) - k_0/k_1 \} \frac{\cosh[x(k_1/D_R)^{1/2}]}{\cosh[x_R(k_1/D_R)^{1/2}]} + k_0/k_1 \quad 0 \leq x < x_R \quad (28)$$

with

$$c(x_R) = c_r + \frac{I_e}{2lb} \{ (x_a - x_i)/D_s + (x_i - x_R)/D_e \} \quad (29)$$

To complete the solution, finally the values of  $k_0$  and  $k_1$  have to be determined. Equations (6) and (7) show that these two quantities are not in-

dependent but are both functions of the overvoltage  $\eta$ . Condition (20) leads to the equation

$$\frac{I_e}{2lb} = -D_R \{c(x_R) - k_0(\eta)/k_1(\eta)\} \tanh[x_R(k_1(\eta)/D_R)^{1/2}] \quad (30)$$

from which the appropriate value of  $\eta$  can be calculated numerically.

### 3.1.2. Tubular plates

In the case of a tubular geometry the most convenient coordinates are cylindrical coordinates. Therefore, the coordinate of our one-dimensional description is the radius  $r$  with the origin at the center of the tube. With the Laplace operator

$$\nabla^2 = \frac{\partial^2}{\partial r^2} + \frac{1}{r} \frac{\partial}{\partial r} \quad (31)$$

we obtain the following differential equations

$$\frac{\partial^2 y}{\partial r^2} + \frac{1}{r} \frac{\partial y}{\partial r} - \frac{k_1}{D_R} y = 0 \quad r_0 \leq r < r_R \quad (32)$$

$$\frac{\partial^2 c_e}{\partial r^2} + \frac{1}{r} \frac{\partial c_e}{\partial r} = 0 \quad r_R \leq r < r_i \quad (33)$$

$$\frac{\partial^2 c_s}{\partial r^2} + \frac{1}{r} \frac{\partial c_s}{\partial r} = 0 \quad r_i \leq r < r_a \quad (34)$$

The surface area  $A$  occurring as a proportionality constant in eqn. (20) is given by

$$A = n_t 2\pi r l, \quad r_R \leq r < r_a \quad (35)$$

Though the finite value of  $r_0$  and the occurrence of the modified Bessel functions make the calculations more tedious, they are basically the same as for flat plates and we obtain

$$c_s = c_r - \frac{I_e}{2\pi l D_s} \ln(r/r_a) \quad r_i \leq r < r_a \quad (36)$$

$$c_e = c_r - \frac{I_e}{2\pi l} \left\{ \frac{1}{D_s} \ln(r_i/r_a) + \frac{1}{D_e} \ln(r/r_i) \right\} \quad r_R \leq r < r_i \quad (37)$$

$$c_R = C \left\{ I_0[r(k_1/D_R)^{1/2}] + \frac{I_1[r_0(k_1/D_R)^{1/2}]}{K_1[r_0(k_1/D_R)^{1/2}]} K_0[r(k_1/D_R)^{1/2}] \right\} + \frac{k_0}{k_1} \quad r_s \leq r < r_R \quad (38)$$

where  $I_N[z]$  and  $K_N[z]$  are modified Bessel functions and the constant  $C$  is given by

$$C = \left\{ c_T - \frac{I_e}{2\pi l} \left[ \frac{1}{D_s} \ln(r_i/r_a) + \frac{1}{D_e} \ln(r_R/r_i) \right] - \frac{k_0}{k_1} \right\} / \left\{ I_0[r_R(k_1/D_R)^{1/2}] + \frac{I_1[r_0(k_1/D_R)^{1/2}]}{K_1[r_0(k_1/D_R)^{1/2}]} K_0[r_R(k_1/D_R)^{1/2}] \right\} \quad (39)$$

Just as in the case of the flat plate, the solution of the problem is completed by numerically determining the value of the overvoltage  $\eta$  according to the boundary conditions. The equation to be solved for  $\eta$  is

$$\frac{I_e}{n_1 2\pi l r_R} = -[k_1(\eta)D_R]^{1/2} C(\eta) \times \left\{ I_1[r_R(k_1(\eta)/D_R)^{1/2}] - \frac{I_1[r_0(k_1(\eta)/D_R)^{1/2}]}{K_1[r_0(k_1(\eta)/D_R)^{1/2}]} K_1[r_R(k_1(\eta)/D_R)^{1/2}] \right\} \quad (40)$$

### 3.2. Evolution with time

In Section 2 it was shown that the discharge process is associated with changes of certain quantities. However, the evolution with time of our model can only be treated numerically. We use an approximation based on the steady state solutions discussed above. As long as the characteristic times of the diffusion processes are small compared with the time of discharge  $t_d$ , short time intervals may be described approximately by steady state solutions. The validity range of this approximation is expressed more precisely by Einstein's equation  $t_d \gg d^2/2D$ , where  $d$  is a characteristic length and  $D$  the diffusion coefficient.

Keeping this limitation in mind we calculate discharge capacities by the following steps:

(i) At the beginning of discharge ( $t = 0$ ) the electrode is fully charged, which means  $z_R = z_i$ , and  $u(z, 0) = u_0$  for  $z_0 \leq z < z_R$ ; the acid concentration is homogeneous having the value  $c(z, 0) = c_0$ . The porosity of the active material is calculated from the amount of active material, the density of  $\text{PbO}_2$  or  $\text{Pb}$ , respectively, and the geometric data of the plate. The zone of active material,  $z_0 \leq z < z_R$ , is divided into a number of layers.

(ii) According to the porosities in the different regions, the acid concentration in the acid reservoir and the current  $I_e$ , a steady state solution is calculated. This is characterized by a certain overvoltage  $\eta$  (diffusion polarization). As long as  $|\eta| < \eta_d$ , where  $\eta_d$  is a predetermined value to define the end of discharge, step (iii) follows. In the case of  $|\eta| \geq \eta_d$  step (iii) is omitted and the calculations are terminated by step (iv).

(iii) By means of this steady state solution the effects of the discharge on the acid concentration in the acid reservoir (eqn. (9)), the active material porosity (eqn. (15)) and the capacity function  $u(z, t)$  (eqn. (13)) are calculated for a short period of time  $\Delta t$ . When the average value of  $u(z, t)$  for a

layer reaches the value 0, this layer is considered to be exhausted and then appears only as a diffusion resistance;  $z_R$  is reduced correspondingly.

Due to this method of calculation the profile of the acid concentration within the region  $z_0 \leq z < z_a$  changes discontinuously. The active material balance, *i.e.*,  $u(z, t)$  has to be corrected for the electrochemical capacity equivalent of these discontinuous changes.

With the new values of  $c_r$ ,  $z_R$ ,  $\pi_R$  (and  $\pi_e$ ) we go back to step (ii) provided there is at least one layer of active material still not exhausted. When all the active material is discharged, the calculations are finished by step (iv).

(iv) The capacity can be calculated either from a summation of the discharge currents and the discharge times of individual steps plus the corrections for the discontinuous changes of the acid concentration profile, or from a total acid balance.

As stated above, there are fitting constants hidden in the model: the porosity of the separator  $\pi_s$ , the effective bulk diffusion coefficient  $D_0$ , and the exponent  $\gamma$  appearing in eqn. (4). To arrive at the modelling of a special cell type, these parameters have to be determined. This may be done by calculating those values of  $\pi_s$ ,  $D_0$ ,  $\gamma$  which, in the sense of least squares, result in the best representation of the capacity/current function characteristic of this cell type. Alternatively, the capacity as a function of some other parameter can be used for this purpose, but very frequently the necessary data will not be available. Using modern computers, such a numerical multiparameter least square fit can be performed by means of standard programs.

#### 4. Results

Having developed the general formalism, we now illustrate the model with a few examples. Despite the question whether tubular or flat plates are considered, the number,  $n_+$ , of positive plates in the model cell is 5. The negative electrode is assumed to have a surplus of capacity, which corresponds to usual traction batteries in which the capacity is positive limited. A standard set of parameters, Table 1, is used throughout the calculations.  $\eta_d = 200$  mV is assumed to be the critical diffusion polarization at which further discharge is prevented by acid depletion inside the porous electrode.

Figure 2 illustrates the two alternative criteria used to define the end of discharge. The development of the diffusion polarization with the depth of discharge is shown for three different discharge currents. In this special example acid balance is capacity limiting only at the rather high discharge current of 130 A. For the two other discharge currents, 10 A and 80 A, the critical diffusion polarization is not reached and in these cases the discharge process is terminated by local exhaustion of the active material.

TABLE 1  
List of symbols and numerical values of several constants used in the calculations of Section 4

| Symbol                                     | Definition   | Value                  | Unit                                     |
|--|--|------------------------|--|
| $b$  | Electrode width  | 23.7                   | cm                                       |
| $c = c(r, t), c(x, t) \text{ or } c(z, t)$ | Acid concentration (indices are used to distinguish between different regions; see Fig. 1)                   | variable               | A h cm <sup>-3</sup>                     |
| $c_0 = c(t = 0)$                           | Initial homogeneous acid concentration   | variable               | A h cm <sup>-3</sup>                     |
| $c^*$                                      | Characteristic constant in $f(i, c)$   | 0.146                  | A h cm <sup>-3</sup>                     |
| $D_0$                                      | Bulk diffusion coefficient   | $3.603 \times 10^{-2}$ | cm <sup>2</sup> h <sup>-1</sup>          |
| $D_j$                                      | Effective diffusion coefficient for the region $j$   | variable               | cm <sup>2</sup> h <sup>-1</sup>          |
| $2d$                                       | Thickness of flat plates   | variable               | cm                                       |
| $F$  | Faraday constant   | 26.802                 | A h mole <sup>-1</sup>                   |
| $f(i, c)$                                  | Active material utilization factor   | variable               | 1  |
| $G$  | Amount of active material of the limiting polarity (Pb or PbO <sub>2</sub> ) in the cell                     | variable               | g  |
| $I$  | Discharge current per cell   | variable               | A  |
| $I_e$                                      | Discharge current per plate of the limiting polarity   | variable               | A  |
| $i = i(r, t), i(x, t) \text{ or } i(z, t)$ | Local specific current   | variable               | A cm <sup>-3</sup>                       |
| $i_0$                                      | Specific exchange current  | $1 \times 10^{-3}$     | A cm <sup>-3</sup>                       |
| $k_0$                                      | Kinetic constant   | variable               | A cm <sup>-3</sup>                       |
| $k_1$                                      | Kinetic constant   | variable               | h <sup>-1</sup>                          |
| $l$  | Electrode length   | 22.8                   | cm                                       |
| $n_+$                                      | Number $\left\{ \begin{array}{l} \text{of positive plates} \\ \text{of negative plates} \end{array} \right.$ | 5                      | 1  |
| $n_-$                                      |  | -                      | 1  |
| $n$  | Number of plates of the limiting polarity  | 5                      | 1  |
| $n_t$                                      | Number of tubes per plate  | 25                     | 1  |
| $r_1$                                      | Inner radius of the tubes  | 0.4                    | cm                                       |
| $r_s$                                      | Spine radius (tubular plates)  | 0.15                   | cm                                       |
| $R$  | Gas constant   | $2.31 \times 10^{-3}$  | A h V K <sup>-1</sup> mole <sup>-1</sup> |
| $t$  | Time   | variable               | h  |
| $t_d$                                      | Discharge time until voltage break-down  | variable               | h  |
| $T$  | Temperature  | 298.15                 | K  |
| $u = u(r, t), u(x, t) \text{ or } u(z, t)$ | Residual capacity per unit volume  | variable               | A h cm <sup>-3</sup>                     |
| $u_0 = u(t = 0)$                           | Initial specific capacity  | 0.145                  | A h g <sup>-1</sup>                      |

|                       |   |          |                             |
|-----------------------|---|----------|-----------------------------|
| $V_a$                 | Total electrolyte volume  |          |                             |
| $V_e$                 | Active electrolyte volume per plate of the limiting polarity  | variable | $\text{cm}^3$               |
| $V_f$                 | Acid reservoir volume per plate of the limiting polarity  | variable | $\text{cm}^3$               |
| $V_R$                 | Volume of the reaction zone   | variable | $\text{cm}^3$               |
| $V_s$                 | Inactive electrolyte volume   | 200      | $\text{cm}^3$               |
| $r, x, z$             | Radial, cartesian and generalized coordinates, respectively   | variable | $\text{cm}$                 |
| $r_j, x_j, z_j$       | Radial, cartesian and generalized coordinates, respectively, of the boundaries between different regions (see Fig. 1) | variable | $\text{cm}$                 |
| $\alpha$              | Transfer coefficient  | 0.5      | 1                           |
| $\gamma$              | Adjustable parameter in expression (4)  | 1.941    | 1                           |
| $\delta_s$            | Thickness of tube walls or separator  | 0.03     | $\text{cm}$                 |
| $\eta$                | Overvoltage   | variable | $\text{mV}$                 |
| $\eta_d$              | Critical overvoltage defining the end of discharge  | 200      | $\text{mV}$                 |
| $\nu$                 | Characteristic constant in $f(i, c)$  | 0.0024   | $\text{cm}^3 \text{A}^{-1}$ |
| $\pi_j$               | Porosity of the region $j$  | variable | 1                           |
| $\pi_s$               | Porosity of the tube wall material  | 0.56     | 1                           |
| $\rho_{20}$           | Electrolyte density, taken at 20 °C   | variable | $\text{g cm}^{-3}$          |
| $\rho_{\text{PbO}_2}$ | Density of $\text{PbO}_2$   | 9.6      | $\text{g cm}^{-3}$          |

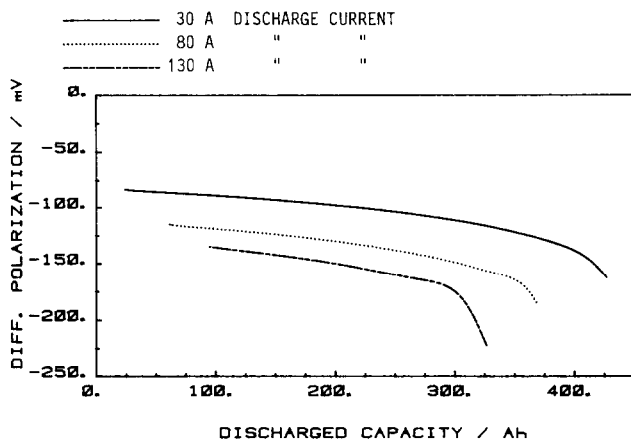


Fig. 2. Calculated diffusion polarizations as function of the degree of discharge. Influence of the discharge current. Model cell with tubular plates;  $V_a = 4.0 \text{ dm}^3$ ;  $V_s = 0.2 \text{ dm}^3$ ;  $\rho_{20} = 1.28 \text{ kg dm}^{-3}$ ;  $G = 880 \text{ g}$ .

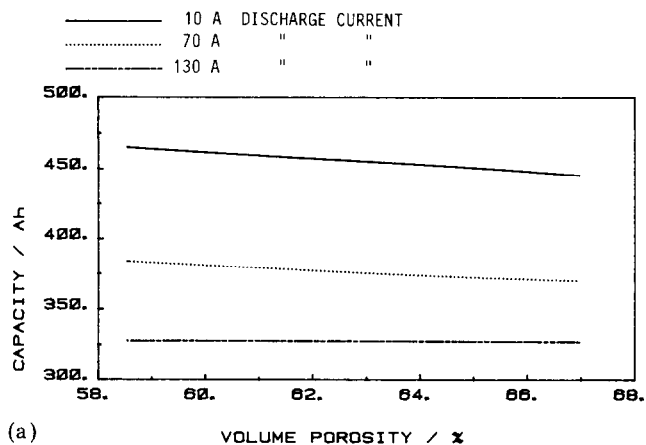
#### 4.1. The influence of the active material porosity

A further example showing the competitive influence of the two limiting mechanisms is given in Fig. 3(a), where the capacity of a model cell with tubular plates is plotted as a function of the active material porosity. Since the electrode volume is fixed, an increased porosity means a reduced amount of active material. Furthermore, increasing the porosity results in a larger amount of acid in the pore system and in a larger effective diffusion coefficient (see eqn. (4)). As can be seen from this Figure, in the case of low or intermediate discharge currents the capacity decreases with increasing porosity. This reflects the decrease in the available amount of active material. Acid balance is of minor importance in this region as at these low currents the acid transport is fast enough. However, the relative importance of the acid balance increases with increasing discharge current. At 130 A the effect of reducing the amount of active material is compensated by a better supply of acid and the capacity becomes practically independent of the porosity.

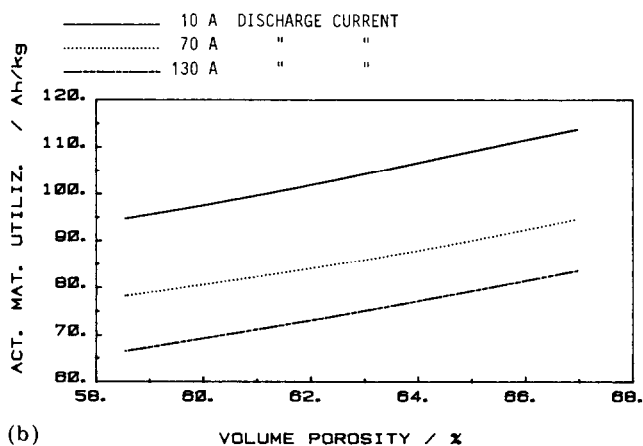
Referring to Fig. 3(b) it should be noted, however, that the active material utilization, which is important for economic considerations, monotonically increases with the active material porosity.

#### 4.2. The influence of the acid volume

In Fig. 4 the discharge capacity is plotted as a function of the amount of electrolyte in the cell for three values of the discharge current. Generally, the capacity increases with increasing amount of acid, as is well known, as a consequence of an increasing average concentration at the electrode surface. While the effect is rather marked at small values of the acid volume  $V_a$ , this dependency becomes weaker with increasing  $V_a$ , and at a discharge current



(a)



(b)

Fig. 3. The discharge capacity (a) and the active material utilization (b) as functions of the initial volume porosity of the active material. Influence of the discharge current. Model cell with tubular plates;  $V_a = 4.0 \text{ dm}^3$ ;  $V_s = 0.2 \text{ dm}^3$ ;  $\rho_{20} = 1.28 \text{ kg dm}^{-3}$ .

of 130 A the capacity seems to reach a stable value for large amounts of electrolyte.

This influence of the discharge current can be qualitatively understood by consideration of the two limiting cases: If the current is very small, the diffusional transport of acid into the porous electrode is relatively fast and thus the acid concentration inside the electrode is strongly coupled to the concentration in the acid reservoir. Therefore, a strong dependency of the capacity on the amount of electrolyte results; the acid capacity controls the cell capacity in this case. A limiting value is reached when the acid volume is so large that the concentration in the reservoir is practically constant during discharge. (Effects of ohmic resistances in the electrolyte are neglected in this consideration.) If, on the other hand, the discharge current is very high, a decoupling of the acid reservoir and the electrolyte inside the porous

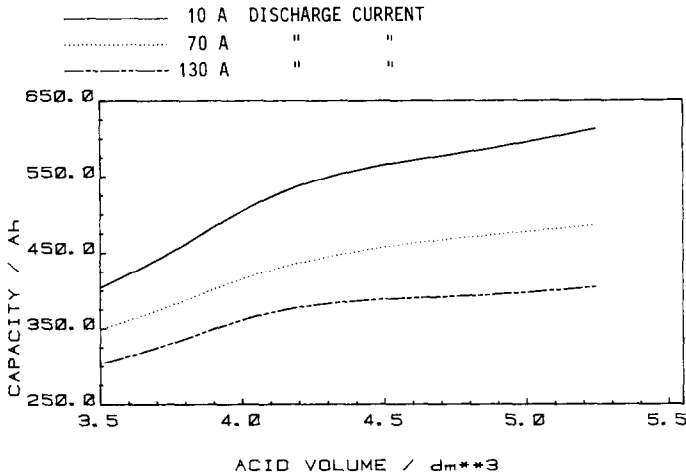


Fig. 4. The discharge capacity as function of the acid volume. Influence of the discharge current. Model cell with tubular plates;  $V_s = 0.2 \text{ dm}^3$ ;  $\rho_{20} = 1.28 \text{ kg dm}^{-3}$ ;  $G = 880 \text{ g}$ .

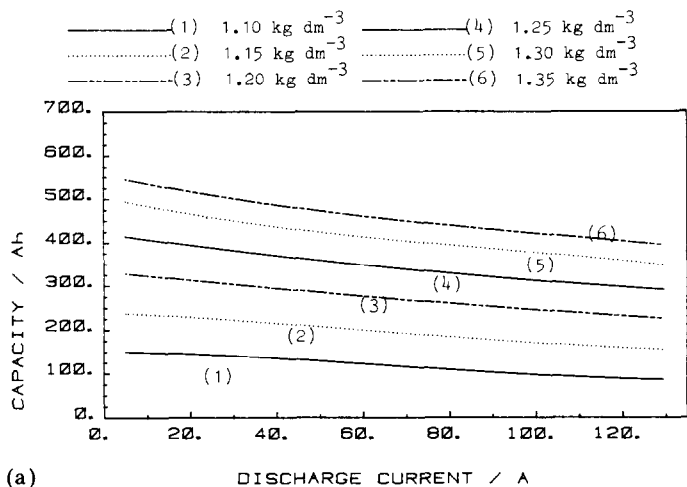
active material results as a consequence of the relatively slow diffusional transport of acid. Thus, in the limiting case, an increased amount of acid has almost no effect on the discharge capacity.

Two situations, in which the influence of the acid volume differs, are discussed in the following examples:

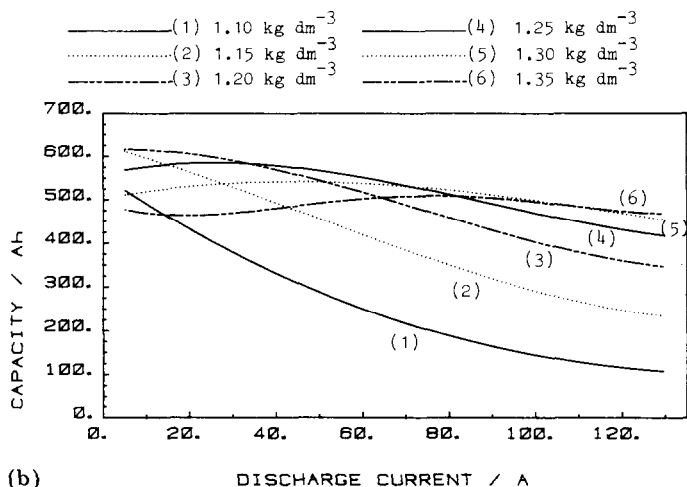
Firstly cell configurations with an acid volume typical of a traction cell are considered. This case is usually characterized by an acid concentration in the reservoir which varies during discharge. Secondly, for comparison, configurations with a large surplus of electrolyte ( $100 \text{ dm}^3$ ), where the concentration in the acid reservoir is practically constant during discharge, are considered. Experimentally this could be realized by pumping electrolyte from a large reservoir through the cell. It seems worthwhile to discuss this as the limiting case for conventional cell designs. Further improvement of the transport of acid requires forced flow of electrolyte through the porous active materials [13].

#### 4.3. The influence of the discharge current

Figure 5 presents the discharge capacity as a function of the discharge current for six values of the acid density. Figure 5(a) (usual amount of electrolyte) shows the small monotonic decrease of capacity with increasing current, which is well known from practical lead-acid cells. A comparison of the curves 1 - 6 shows that, in accordance with practical experience, an increased acid density results in a larger capacity. The situation is much more complicated in Fig. 5(b) (large surplus of acid). Here, in general, the capacity/current functions show a maximum. The current value corresponding to this maximum is a function of the acid density; with increasing acid density the maximum is shifted to higher discharge currents. As a consequence, an increased acid density does not always imply a larger capacity.



(a)



(b)

Fig. 5. The discharge capacity as a function of the discharge current. Influence of the acid density. (a):  $V_a = 4.0 \text{ dm}^3$  (usual cell design). (b):  $V_a = 100 \text{ dm}^3$  (large surplus of electrolyte). Model cell with tubular plates;  $V_s = 0.2 \text{ dm}^3$ ,  $G = 880 \text{ g}$ ; acid densities (taken at  $20^\circ \text{C}$ ) as indicated in the legends.

These results indicate the complicated interrelations between the different influences. A qualitative explanation is based on eqns. (13), (14), which describe the local active material utilization as a function of the time dependent values of the local acid concentration and the current density as derived from ref. 13. With respect to the acid density, the function  $f(i, \rho)$  has a maximum at an acid density  $\rho_{\max} = 1.16 \text{ kg dm}^{-3}$ . To get a feeling of the much more complicated dependency of the active material utilization of an electrode as a whole, it is helpful to consider an appropriately averaged acid density,  $\bar{\rho}$ . The average has to be taken over the discharge time and the extension of the active material. Though this average is not

simple to calculate, the results of Section 3 show that  $\bar{\rho}$  decreases with increasing current and with decreasing acid density. In this way Fig. 5(b) reflects the influence of eqn. (14) on the capacity of the electrode. The reason that maxima are not observed in Fig. 5(a) is the limited acid volume, a consequence of which is a marked decrease of the acid concentration in the reservoir during discharge. Therefore, in all the situations covered by Fig. 5(a) the resulting values of  $\bar{\rho}$  are less than  $\rho_{\max}$ .

#### 4.4. The influence of the electrode thickness

Model cells with flat plates are considered in the following two examples. The influence of the discharge current together with the influence of the plate thickness on the active material utilization is shown in Fig. 6. As in the previous example (4.3.), the active material utilization of a model cell with a usual amount of electrolyte (Fig. 6(a)) decreases with increasing specific current. Reducing the plate thickness results in an improvement in the active material utilization. Again, as in Section 4.3., the situation is completely different if a cell with a constant acid concentration in the reservoir is considered (Fig. 6(b)). Just as in Fig. 5(b), a maximum is observed in the active material utilization *versus* current curves. With decreasing plate thickness the maximum moves to higher values of the discharge current.

Analogous to the discussion of Fig. 5, these results can be interpreted in terms of the averaged acid density  $\bar{\rho}$ . As can be seen from Section 3,  $\bar{\rho}$  depends also on the plate thickness: with decreasing plate thickness  $\bar{\rho}$  increases. This fact together with eqn. (14) results in an influence of the plate thickness on the average active material utilization. The maxima occurring in Fig. 6(b) reflect the dependence of the utilization factor  $f(i, c)$  on the acid concentration.

#### 4.5. The influence of the acid density

Figure 7 shows the influence of acid density and plate thickness on the active material utilization. Both parameters strongly influence the value of  $\bar{\rho}$ . In the case of a cell with a usual amount of electrolyte (Fig. 7(a)) a maximum of the active material utilization *vs.* acid density function only appears for the rather thin, 1.5 mm thick, plate. According to eqn. (14) and the discussion above, in the case of thicker plates maxima are expected at higher values of the acid density. These tendencies are even more pronounced in the case of acid surplus, as can be seen from Fig. 7(b).

In order to make a comparison with data in the literature, a different representation is given in Fig. 8: The active material utilization *vs.* acid concentration curve is shown for different values of the specific discharge current. Comparison with Figs. 4.10 and 4.11 of Bode [15], in which flat plates of 1.1 and 4.4 mm plate thickness are considered, shows that within the validity range of our model the results agree well with practical experience.

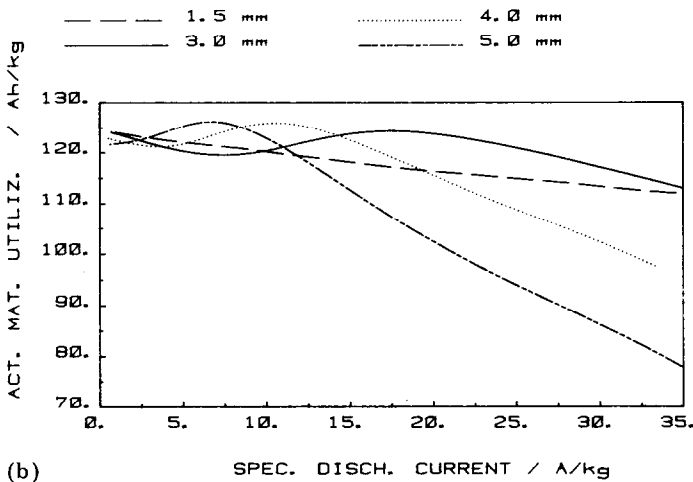
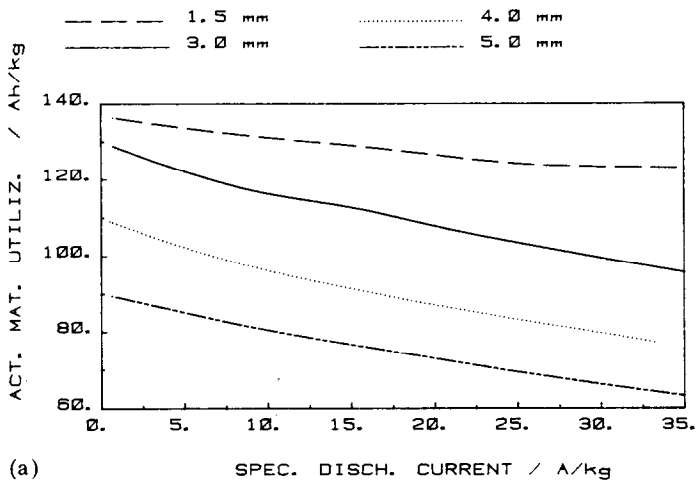


Fig. 6. The active material utilization as a function of the specific discharge current. Influence of the plate thickness. (a):  $V_a = 3.6 \text{ dm}^3$  (usual cell design). (b):  $V_a = 100 \text{ dm}^3$  (large surplus of electrolyte). Model cell with flat plates;  $V_s = 0.2 \text{ dm}^3$ ;  $\rho_{20} = 1.28 \text{ kg dm}^{-3}$ ; initial volume porosity of the active material = 0.63; plate thickness as indicated in the legends.

## 5. Conclusion and discussion

A method for the calculation of the discharge capacity of lead-acid cells based on the macrohomogeneous model has been developed. Approximations were introduced to obtain a model which can be easily handled. Acid transport, described by an effective diffusion process, was considered to be the crucial influence except at high discharge currents. The model contains adjustable parameters, which are assumed to account for convective

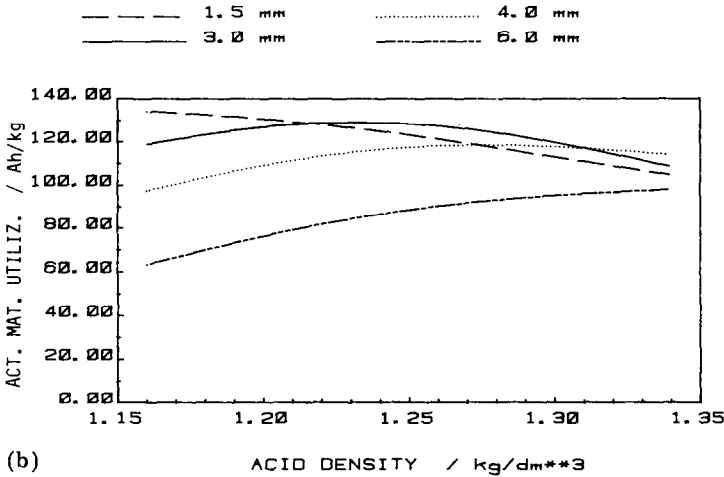
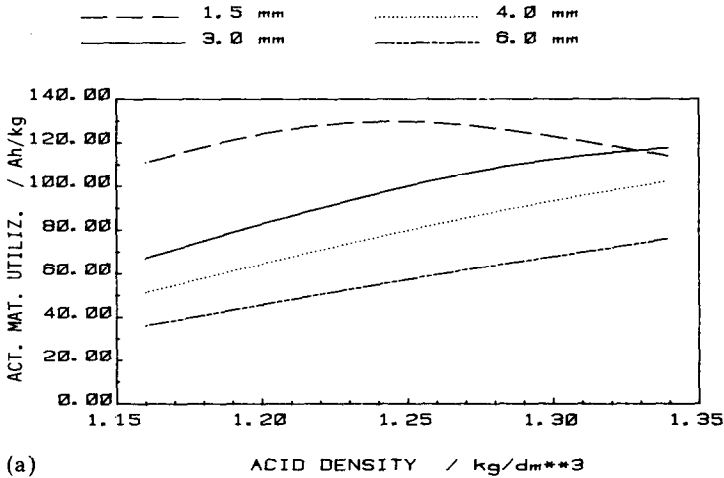


Fig. 7. The active material utilization as a function of the acid density. Influence of the plate thickness. (a):  $V_a = 3.6 \text{ dm}^3$  (usual cell design). (b):  $V_a = 100 \text{ dm}^3$  (large surplus of electrolyte). Model cell with flat plates;  $V_g = 0.2 \text{ dm}^3$ ; specific discharge current =  $91 \text{ A kg}^{-1}$ ; initial volume porosity of the active material = 0.63; plate thickness as indicated in the legends.

and migrational transport of acid and which allow the model to be adapted to particular cell types. The model has been worked out for flat as well as for tubular plates. The value of the proposed model is demonstrated by several examples treating the dependence of the capacity or the active material utilization on the discharge current, the acid density, the amount of electrolyte, the active material porosity, and the plate thickness. The examples discussed show that a model is now available which allows a detailed understanding of the capacity determining mechanisms found in practical cells. This is clearly demonstrated by comparison of Fig. 8 with the

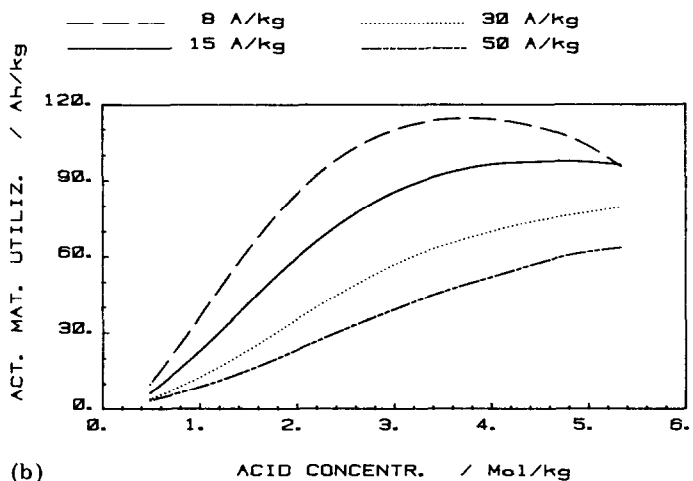
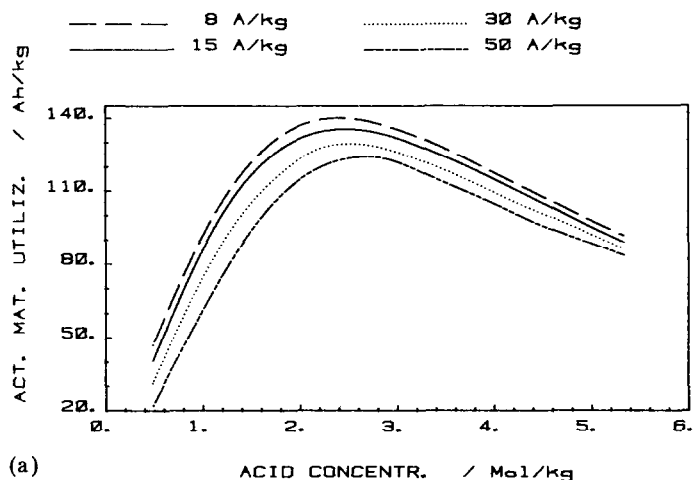


Fig. 8. The active material utilization as a function of the acid concentration. Influence of the specific discharge current (see the legends) and of the plate thickness: 0.11 cm in (a) and 0.44 cm in (b). Model cell with flat plates:  $V_a = 100 \text{ dm}^3$ ;  $V_s = 0.2 \text{ dm}^3$ ; initial volume porosity of the active material = 0.54.

corresponding practical data given by Bode [15]. Therefore, this model is useful for the design and optimization of lead-acid cells.

With regard to previous applications of the macrohomogeneous model, it is of interest to consider the acid concentration profiles that develop during discharge. Earlier calculations [4, 14] gave physically unrealistic results with the lowest values of the acid concentration at the electrode surface. Due to the proper boundary conditions, the present model is in accordance with a realistic acid distribution, as discussed by Micka and Roušar [5].

Improvements in the present approach will have to take into consideration the ohmic effects in the grids, the active material, and the electrolyte. Furthermore, an explicit treatment of the time evolution of the acid concentration would enable the model to be extended to high discharge currents. A correlation of the present model with the previously described treatment of the capacity of strongly relaxing electrochemical systems [16], and an application to the charging process, seem also to be worthwhile.

## References

- 1 R. W. Burrows and H. R. Espig, *J. Power Sources*, 4 (1979) 291.  
D. A. J. Rand, *J. Power Sources*, 5 (1980) 221.  
E. Voss, *J. Power Sources*, 7 (1982) 343.
- 2 W. H. Tiedemann, J. Newman and F. Desua, in D. H. Collins (ed.), *Power Sources 6*, Academic Press, New York, 1977, p. 15.
- 3 J. Newman and W. Tiedemann, *AIChE J.*, 21 (1975) 25.
- 4 K. Micka and I. Roušar, *Electrochim. Acta*, 18 (1973) 629.
- 5 K. Micka and I. Roušar, *Collect. Czech. Chem. Commun.*, 40 (1975) 921; *Electrochim. Acta*, 21 (1976) 599.
- 6 N. A. Hampson and J. B. Lakeman, *J. Power Sources*, 6 (1981) 101.
- 7 W. Stein, *Dissertation*, Techn. Hochschule Aachen, 1959.
- 8 H. Lehning, *Electrotech. Z. Ausg. A*, 93 (1972) 62.
- 9 P. Horváth, in J. Thompson (ed.), *Power Sources 9*, Academic Press, London, 1983.
- 10 R. Pollard and J. Newman, *J. Electrochem. Soc.*, 128 (1981) 491.
- 11 W. Kappus and A. Winsel, *J. Power Sources*, 8 (1982) 159.
- 12 K. Asai, M. Tsubota, K. Yonezu and K. Ando, *J. Power Sources*, 7 (1981) 73.
- 13 U. Hullmeine and W. Kappus, *Electrochim. Acta*, 27 (1982) 1677.
- 14 D. Simonsson, *J. Appl. Electrochem.*, 3 (1973) 261.
- 15 H. Bode, *Lead-Acid Batteries*, Wiley, New York, 1977.
- 16 W. Kappus and U. Hullmeine, *Electrochim. Acta*, 26 (1981) 1103.